nature sustainability

Article

https://doi.org/10.1038/s41893-025-01620-x

Ecological risk assessment of marine plastic pollution

Received: 10 October 2024

Accepted: 28 July 2025

Published online: 02 September 2025

Check for updates

Ziman Zhang[1], Peipei Wu[2], Xinle Wang[1], Qiaotong Pang[1], Yujuan Wang[1], Xianming Zhang[3], Karin Kvale[4], Eddy Y. Zeng[5], Lili Lei[1] & Yanxu Zhang[6]

Plastic pollution poses serious ecological risks to marine organisms through various pathways, yet a comprehensive risk assessment is lacking. Here we assess the global risks of plastic ingestion, entanglement, pollutant adsorption (methylmercury, MeHg; perfluorooctane sulfonate, PFOS) and additive leaching (bisphenol A; phthalate esters) by integrating a marine plastic model and multisize marine organism data, as well as MeHg and PFOS datasets. Our analysis reveals that ingestion risks vary with the body size of organisms, and are influenced by both biomass distribution and plastic concentration patterns. Entanglement hotspots align with regions of flourishing coastal fisheries, highlighting a substantial threat to marine species. Ingestion risks and toxicity from leached additives are concentrated in the mid-latitude North Pacific Ocean, mid-latitude Atlantic Ocean and northern Indian Ocean. Plastics exhibit high adsorption of PFOS in the North Atlantic and East and Southeast Asian coasts (0.1–0.3 pg m^{-2}) and of MeHg in the northern Indian and southwestern Atlantic oceans (1–18 pg m^{-2}). Using future emission scenarios, we project plastic concentrations and estimate reduced risks under emission control strategies. These findings emphasize the urgent need for targeted mitigation efforts and policy interventions to curb escalating impacts of plastic pollution on marine ecosystems.

Marine plastic pollution has emerged as one of the most pressing global environmental challenges[1]. Each year, millions of tons of plastics enter the ocean from rivers, coastlines, shipping and fishing[2]. These plastics disperse throughout the marine environment, reaching ocean gyres and even polar regions, and pose serious threats to marine ecosystems[3].

The ecological impacts of marine plastic pollution are complex and multifaceted. Numerous studies have documented plastic ingestion by marine organisms[4]. Plastic debris has been identified in the gastrointestinal tracts of diverse marine species, including fish, turtles, seabirds and other fauna[5,6]. Ingesting plastics can lead to various detrimental effects, such as intestinal blockage and false satiety[7]. These biological consequences extend to altered feeding behaviour, reduced body condition and increased mortality[8]. The probability of ingestion risk is intricately linked to numerous factors such as habitat, body size and ingestion rate[9,10]. There is also a positive correlation between the body length of marine animals and the maximum size of plastic they are capable of ingesting[11]. For example, the standard length of fish is positively associated with the number of particles found in the gastrointestinal tract[12].

Plastics can entangle the necks and limbs of wildlife, causing behavioural disturbances and physical injuries, which may be more lethal than ingestion, as evidenced by numerous field observations[4,13]. Various types of plastic, including ropes, bags, tyres and especially abandoned, lost and discarded fishing gear (ALDFG, known as ghost

[1]School of Atmospheric Sciences, Nanjing University, Nanjing, China. [2]Scripps Institution of Oceanography, University of California San Diego, La Jolla, CA, USA. [3]Department of Chemistry and Biochemistry, Concordia University, Montreal, Quebec, Canada. [4]Aotearoa Blue Ocean Research, Lower Hutt, New Zealand. [5]School of Environment and Energy, South China University of Technology, Guangzhou, China. [6]Department of Earth and Environmental Sciences, Tulane University, New Orleans, LA, USA. e-mail: yzhang127@tulane.edu

https://doi.org/10.1038/s41893-025-01620-x

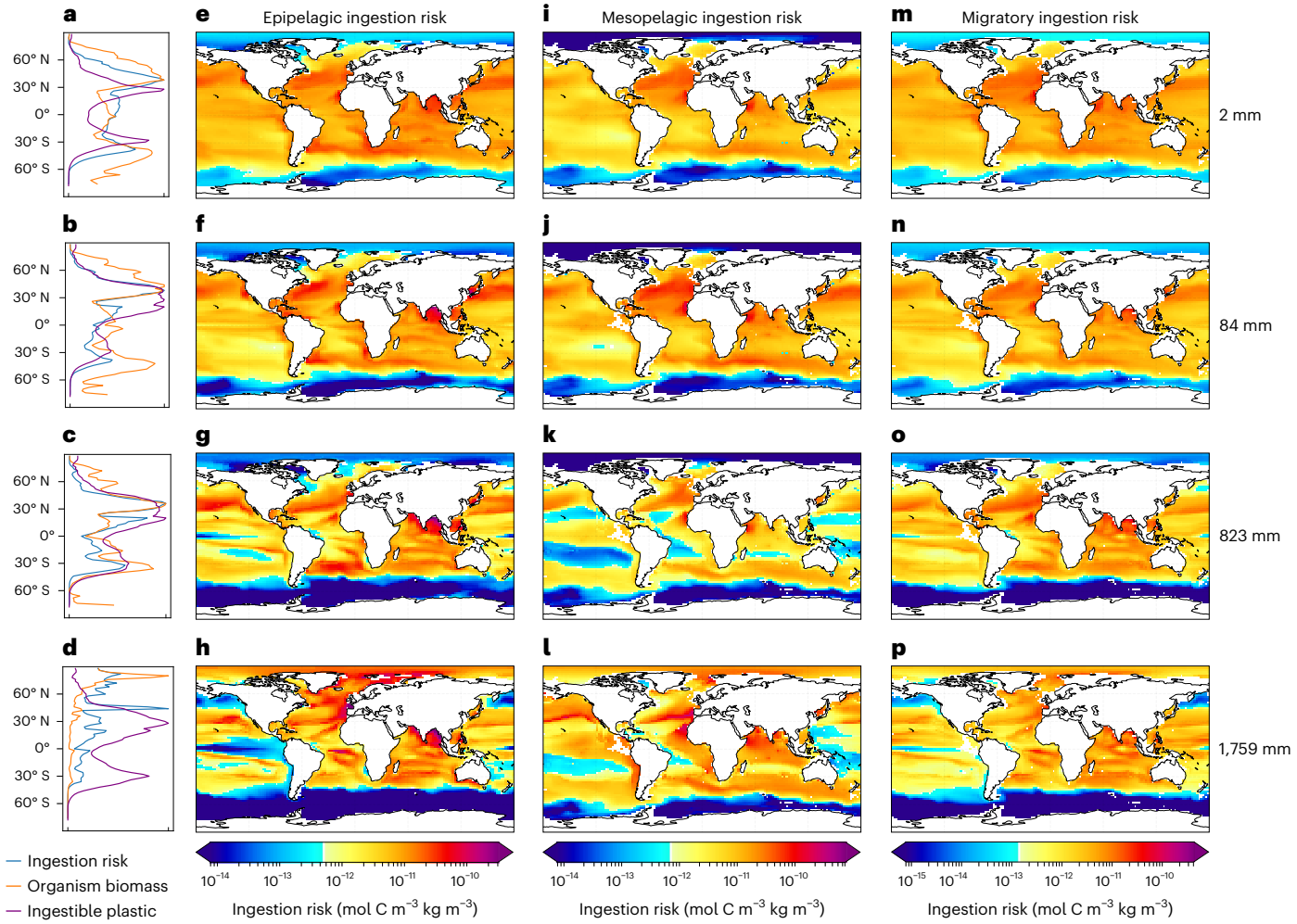

Fig. 1 | Plastic ingestion risk by marine organism size and type. a–d, The latitudinal distribution of mean normalized ingestion risk, biomass and ingestible plastic concentrations for epipelagic organisms of different body sizes: 2 mm (**a**); 84 mm (**b**); 823 mm (**c**); 1,759 mm (**d**). **e–h**, Global distribution of plastic ingestion risk for epipelagic organisms: 2 mm (**e**); 84 mm (**f**); 823 mm (**g**); 1,759 mm (**h**). **i–l**, Global distribution of plastic ingestion risk for mesopelagic organisms: 2 mm (**i**); 84 mm (**j**); 823 mm (**k**); 1,759 mm (**l**). **m–p**, Global distribution of plastic ingestion risk for migratory organisms: 2 mm (**m**); 84 mm (**n**); 823 mm (**o**); 1,759 mm (**p**). Basemaps in **e–p** from Natural Earth (https://www.naturalearthdata.com).

fishing), contribute substantially to the entanglement risk[14]. The expansion of fishing activities in recent years has accelerated the prevalence of ghost gear[15], posing heightened threats to marine mammals, reptiles and elasmobranchs[16]. Such a risk shows an age preference, with younger animals being more susceptible to entanglement due to curiosity[17]. Records indicate that organisms experiencing plastic entanglements vary in length, ranging from 25 cm (sea turtles) to over 2 m (whales and seals)[18–20].

Plastics possess the capability to adsorb organic pollutants and metals owing to their hydrophobic nature and large specific surface area[21]. The sorption behaviour is contingent upon factors such as polymer type, particle size and seawater temperature[22]. Persistent toxic pollutants such as methylmercury (MeHg) and perfluorooctane sulfonate (PFOS) can adsorb onto plastics, forming complexes that are susceptible to ingestion by marine organisms and subsequent transfer through trophic levels within food webs[23–25]. Notably, smaller plastic particles tend to accumulate higher concentrations of PFOS than their larger counterparts, probably due to their greater specific surface area[26,27]. Consequently, plastic debris serves as a vector for the horizontal and vertical transport of adsorbed pollutants in the ocean, broadening the spatial extent of exposure[28]. Moreover, plastic degradation releases additive chemicals such as bisphenol A (BPA) and phthalate esters (PAEs), which are used as ultraviolet stabilizers and plasticizers, respectively[29]. These leached chemicals, classified as endocrine disruptors, may impair organismal growth and metabolism, and potentially induce genetic mutations[30]. Current risk assessments are limited by narrow taxonomic focus, restricted geographic scope and incomplete characterization of exposure pathways[9,10,31].

In this Article we propose a comprehensive and scalable framework for assessing the ecological risks of marine plastics at the global scale by quantifying four major exposure pathways: ingestion, entanglement, pollutant adsorption and additive leaching. We utilize plastic concentration outputs from the Nanjing University Marine Plastic (NJU-MP) model within the Massachusetts Institute of Technology general circulation model (MITgcm) framework, which simulates plastic emission, transport and sinking processes, constrained by observational datasets[32]. We also incorporate global marine biomass data from the NEMO-PISCES-APECOSM model, which resolves 20 organism size classes for upper trophic levels[33]. To evaluate pollutant exposure, we use simulated distributions of MeHg and PFOS, selected for their toxicity, persistence and well-characterized physicochemical properties[23,24]. Leaching risks are estimated for common additives such as BPA and PAEs, on the basis of literature-derived data, their widespread use and ecological impacts[34,35]. Due to the absence of quantitative dose–effect relationships specific to marine plastics, we evaluate relative risk probabilities rather than absolute risk levels.

https://doi.org/10.1038/s41893-025-01620-x

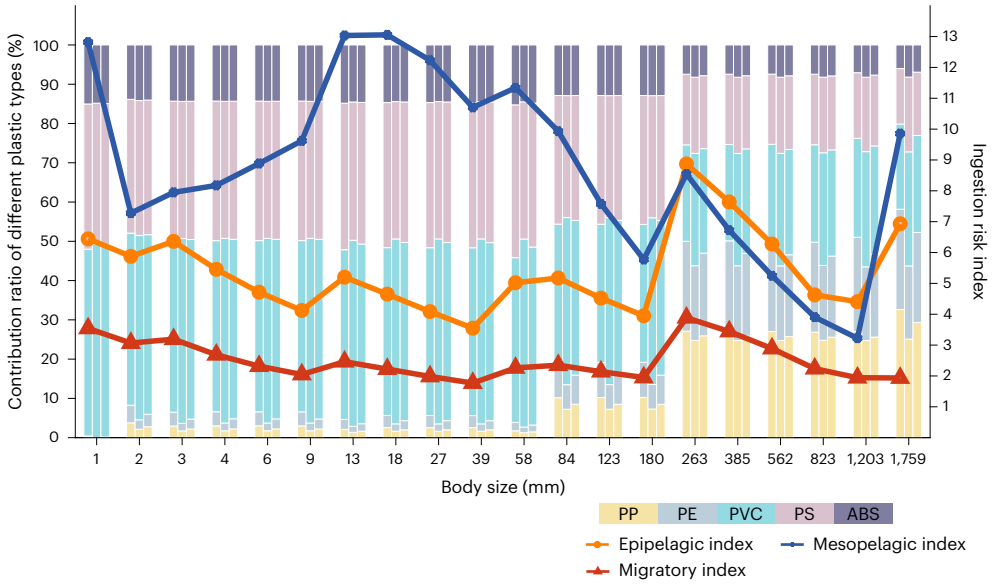

Fig. 2 | Ingestion risk index for varied organisms of different body sizes contributed by different plastic types. The model considers the plastic types PP, PE, PVC, PS and ABS. The three lines represent total ingestion risk for epipelagic organisms, mesopelagic organisms and migratory organisms.

Ingestion risk

The global pattern of plastic ingestion risk varies for organisms of different body sizes (Fig. 1). We calculate ingestion risk probability by multiplying organism biomass by plastic concentrations within ingestible size ranges, followed by zonal summation and normalization to reveal latitudinal patterns (Methods). For epipelagic organisms (2–823 mm), ingestion risk peaks at mid-latitudes (30–50°) and declines in tropical regions (<20°), reflecting the contrasting distributions of biomass and plastics. Modelled plastics accumulate in Asian coastal zones and oligotrophic subtropical gyres, driven by high emissions and surface transport processes such as Ekman convergence and tidal stranding along coastlines[36] (Supplementary Fig. 1). Conversely, biomass is concentrated in eutrophic zones such as current margins, tropical waters and high latitudes (Supplementary Fig. 2). Elevated nutrient availability and phytoplankton productivity in these areas are linked to vertical processes, including upwelling, mixed-layer shoaling and turbulent mixing, which are generally weak in subtropical gyres[37,38]. These differing spatial patterns are supported by significant negative spatial correlations between surface plastic concentrations and nutrient levels (phosphate, nitrate and chlorophyll *a*) across most central subtropical gyres (Supplementary Fig. 3).

The hotspots of modelled ingestion risk are identified in both hemispheres, with particularly high levels in the mid-latitude North Pacific and North Atlantic oceans. Specifically, the northwestern Atlantic exhibits notable ingestion risk for small organisms, contrasting with a heightened risk for large organisms in the northeastern Atlantic (Fig. 1e–p). In the northern Indian Ocean, vertical heterogeneity in plastic distribution leads to high ingestion probabilities for epipelagic organisms in the Bay of Bengal and mesopelagic organisms in the Arabian Sea (Supplementary Fig. 1). In the equatorial Pacific Ocean, mesopelagic organisms face ingestion risks three orders of magnitude higher than do epipelagic and migratory organisms with a body size exceeding 823 mm. In the Southern Hemisphere, higher plastic ingestion risk occurs in the South Atlantic Ocean, the southern Indian Ocean and the upwelling zones (Peruvian cold currents). Although plastic loads are low in these upwelling regions, the abundance of organisms contributes to high risk (Supplementary Fig. 2). Our model reveals that plastic garbage patches and biomass hotspots do not always overlap. In the South Pacific, plastics accumulate around 30° S, whereas organisms are concentrated in the range 30–60° S. As a result, ingestion risk remains low despite the presence of a garbage patch, potentially mitigating the ecological impact. In the Northern Hemisphere, the largest organisms (approximately 2 m) face substantial ingestion risk, particularly in the Arctic Ocean, a key habitat with high biomass of large-bodied species that further elevates this risk (Fig.1d,h,l and Supplementary Fig. 2i–l). The polar branch of the thermohaline circulation has the potential to transport plastics from lower latitudes to the Arctic region, facilitating their sinking and subsequent accumulation[39]. This mechanism raises notable ecological concern. Field observations confirm that fish in the Arctic Ocean are ingesting plastic polymers, including polyethylene (PE) and polyvinyl chloride (PVC), in diverse sizes and colours[40].

We sum the ingestion risk and multiply it by 10^8 to generate a comparable risk index and assess the contributions of various plastic types to organism groups (Fig. 2). Mesopelagic organisms, boasting the largest biomass, contribute the highest total ingestion risk (176), followed by epipelagic organisms (108) and migratory species (50). The highest risk index is 14 for mesopelagic organisms with a body size of 18 mm. Organisms of 1,203 mm have the lowest ingestion risk index (3.2). For epipelagic and migratory groups, peak risk occurs at a body size of 263 mm, with indices of 8.9 and 3.9, respectively. The contribution ratio of different plastic types is influenced by their size distribution and abundance in seawater. Model results suggest that PVC and polystyrene (PS), within the 0.078–0.3-mm size range, are the predominant components in the surface ocean, with global masses of 3.5×10^8 kg and 2.7×10^8 kg, respectively (Supplementary Fig. 4). Consequently, for smaller organisms, PVC poses the highest risk (45.5%), followed by PS (35.7%) and acrylonitrile butadiene styrene (ABS) (14.5%). As organism size increases, the combined contribution of polypropylene (PP) and PE exceeds 50%, consistent with field observations of dominant ingestion by fish ranging from 291 to 707 mm (ref. 41). This pattern probably reflects the lower densities of these polymers relative to seawater, which promote their retention near the surface and constrain vertical transport. In contrast, denser polymers such as PVC, PS and ABS are more prone to sinking and accumulating at greater depths.

Entanglement risk

We assess plastic entanglement risk as the product of macroplastic abundance and organism biomass, representing the probability of interaction between large-bodied organisms (>180 mm) and macroplastics (>5 cm) originating from fishing and shipping sources, such as ALDFG. The

https://doi.org/10.1038/s41893-025-01620-x

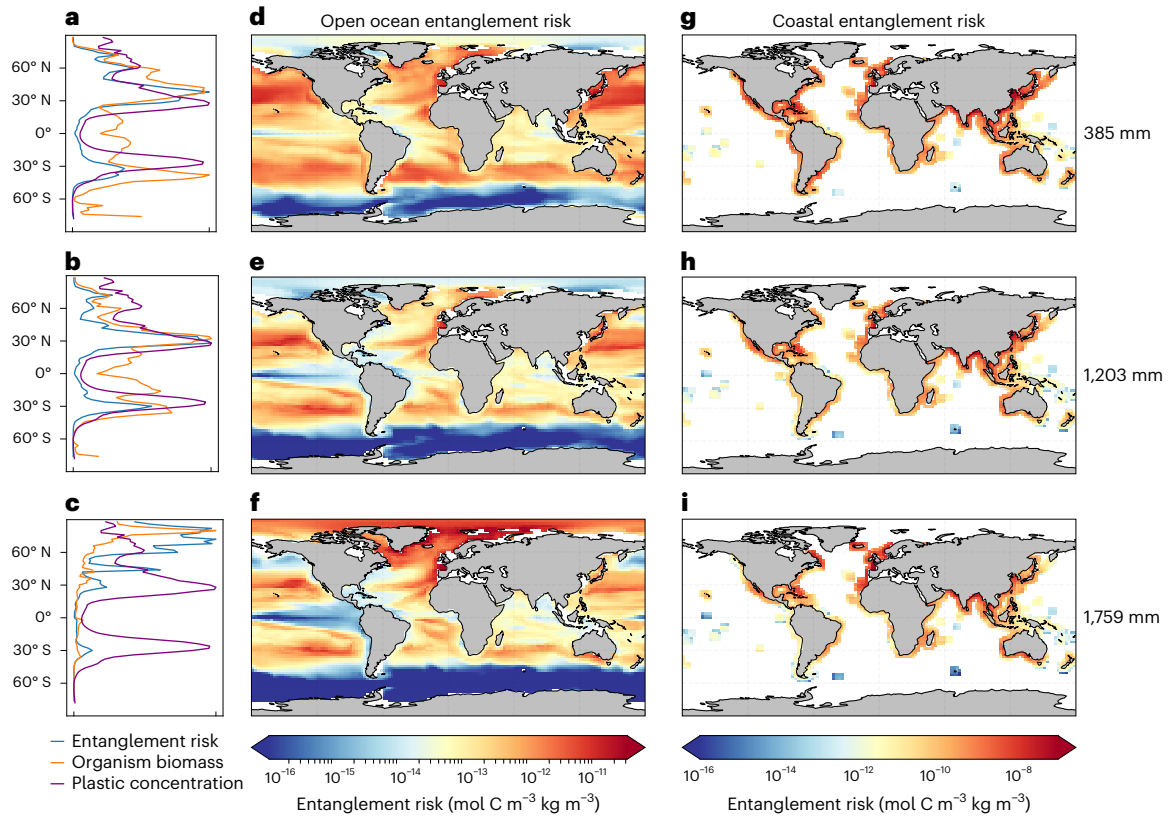

Fig. 3 | Plastic entanglement risk for marine organisms. a–c, Latitudinal distribution of the mean entanglement risk, biomass and ocean-source plastic concentration for organisms of different body sizes: 385 mm (**a**); 1,203 mm (**b**); 1,759 mm (**c**). **d–f**, Global distribution of plastic entanglement risk in the open ocean: 385 mm (**d**); 1,203 mm (**e**); 1,759 mm (**f**). **g–i**, Global distribution of plastic entanglement risk in coastal regions: 385 mm (**g**); 1,203 mm (**h**); 1,759 mm (**i**). Basemaps in **d–i** from Natural Earth (https://www.naturalearthdata.com).

modelled risk suggests two peaks at 30° N and 30° S with a pronounced decline at the equator, reflecting the latitudinal distribution of biomass and plastic concentrations. A distinctive increase in risk for the largest organisms appears north of 40 °N, driven by higher biomass and intensified fisheries and shipping activity in the Arctic Ocean, where ALDFG and other marine debris are abundant[42] (Fig. 3a–c). Major hotspots include the subtropical Pacific, the northeastern and southeastern Atlantic and the southern Indian Ocean near 30 °S (Fig. 3d–f). In contrast to ingestion risk, entanglement risk is lower in the northwestern Atlantic and the Indian Ocean (for example, Gulf of Mexico and Sargasso Sea; Supplementary Fig. 5d) due to low fishing effort and limited ALDFG input[43].

Our results identify coastal regions as prominent hotspots for entanglement risk, driven by frequent fishing activities[44]. Summing entanglement risk and scaling by 10^6, we find that total entanglement risk in coastal regions (18) surpasses that in open oceans (0.039) by over two orders of magnitude. This elevated coastal risk indicates increased entanglement exposure for animals during foraging trips, especially where fishing grounds overlap with densely populated coastlines[45]. High-risk areas include the Sea of Okhotsk, the Sea of Japan, the Yellow Sea of China, the East China Sea, the coastal areas of Southeast Asia and the northernmost Bay of Bengal, all characterized by active fisheries and aquaculture (Supplementary Fig. 6a, b). These patterns are further supported by entanglement incidents involving rays and sharks along the coasts of North America and Australia[46], and high entanglement rates in Hawaii Island, Kaikoura Island and upwelling systems such as the Gulf of California[47] (Supplementary Fig. 6c–e).

Pollutant conveyor risk

The loadings of PFOS and MeHg on plastics, as representative contaminants, are derived assuming thermodynamic equilibrium with seawater and reflect the combined influence of plastic abundance and ambient pollutant concentrations (Methods). The maximum PFOS load absorbed onto plastics is 0.3 pg m^{-2} in the Gulf Stream, driven by the riverine discharge from terrestrial sources into the ocean[48]. Substantial adsorption is also estimated in the North Atlantic and Indian oceans (Fig. 4a). For MeHg, adsorbed plastic loads are higher along the coasts of East and Southeast Asia, the east coast of South America and the Bay of Bengal (1–18 pg m^{-2}) (Fig. 4b). The equatorial oceans and the North Pacific show substantial adsorption. In the Arctic, reduced solar radiation limits demethylation, resulting in high concentrations[49]. MeHg loads are lower than 0.001 pg m^{-2} in the tropical North Atlantic and Indian oceans (<30°), due to a fast photochemical demethylation rate and low biomass[49].

The drifting velocity of surface plastics, governed by wind, ocean currents and particle-specific properties such as density and shape, alters the transport patterns of PFOS and MeHg relative to ocean circulation[32,50]. Drifting velocities are high in the offshore regions of East Asia and Southeast Asia, facilitating predominant eastward transport into the North Pacific. In the northern Sargasso Sea and along the east coast of South America, plastics laden with these pollutants enter the Atlantic Ocean. As drifting velocities can exceed ocean currents, plastics may intensify pollutant flux toward convergence zones and serve as conveyors transporting contaminants from coastal regions to the open ocean (Supplementary Fig. 7). In regions with high pollutant adsorption and plastic ingestion overlap, marine organisms may ingest contaminated plastics, increasing bioaccumulation risks and threatening ecosystems and human health[24,26]. Exposure risk is assessed by multiplying organism biomass by the concentration of contaminants adsorbed onto ingested plastic. High risks are identified for PFOS and MeHg in the North Pacific and North Atlantic, and

https://doi.org/10.1038/s41893-025-01620-x

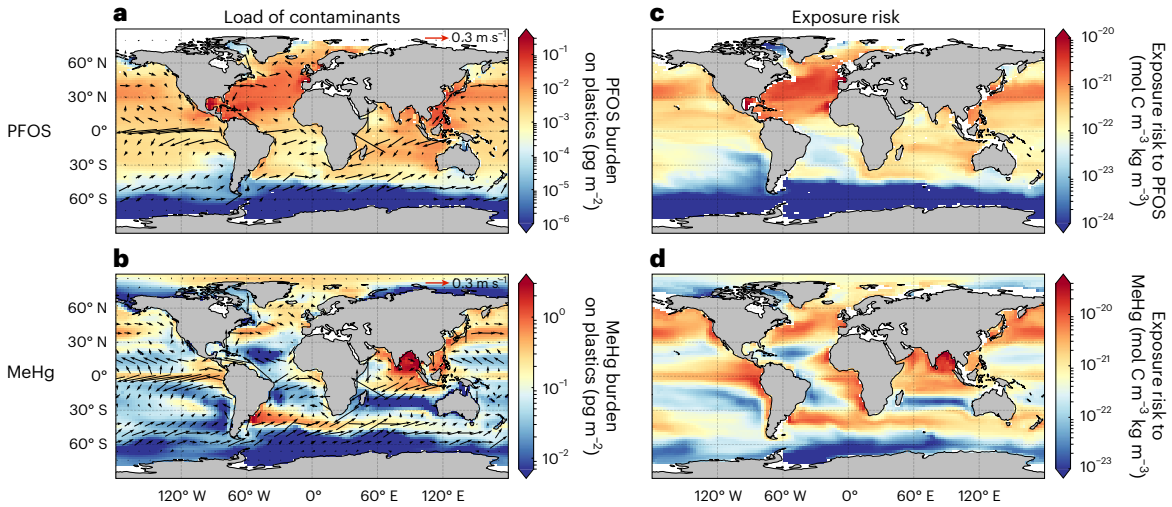

Fig. 4 | Global distribution of and exposure risk of organisms to pollutants adsorbed and conveyed by plastics. a,**b**, Global distribution of PFOS (**a**) and MeHg (**b**) adsorbed and conveyed by plastics. Arrows are drifting velocity of floating plastics driven by the forces of both wind and seawater. **c**,**d**, Exposure risk of organisms to PFOS (**c**) and MeHg (**d**) adsorbed by ingested plastics. Basemaps from Natural Earth (https://www.naturalearthdata.com).

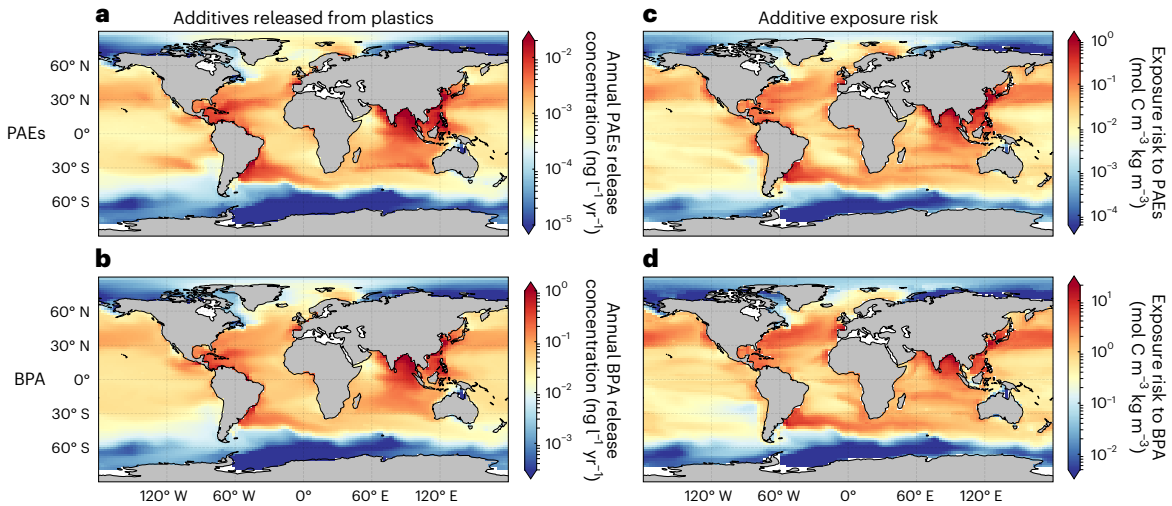

Fig. 5 | Global distributions of leached PAEs and BPA from plastics. a, PAEs leaching from PE, PP and PVC. **b**, BPA leaching from PVC and PS. **c**,**d**, Exposure risk for all organisms to PAEs (**c**) and BPA (**d**) leached from plastic. Basemaps from Natural Earth (https://www.naturalearthdata.com).

for MeHg in the Indian and equatorial Pacific oceans (Fig. 4c,d and Supplementary Figs. 8 and 9).

Additive leaching risk

We calculate the total mass and leaching rates of two representative additives, PAEs and BPA, in marine plastics using reported content levels and leaching rates across polymer types (Extended Data Table 1 and Supplementary Section 1). PVC contains the highest mass of PAEs (5.4×10^7 kg), while BPA is most abundant in PE (4.0×10^6 kg). The global release rates of PAEs and BPA from marine plastics are estimated as 1.9×10^4 and 6.1×10^5 kg yr^{-1}. PVC has the highest PAE leaching rate of 253 μg kg^{-1} d^{-1}, contributing the largest annual release of 1.4×10^4 kg yr^{-1}, followed by PE (4.9×10^3 kg yr^{-1}) and PP (5.6×10^2 kg yr^{-1}). The estimated BPA release is 5.1×10^5 kg yr^{-1} from PS and 1.0×10^5 kg yr^{-1} from PVC, on the basis of experimental leaching rates[51,52].

We estimate the contributions of marine plastics to surface ocean concentrations of PAEs and BPA (Fig. 5). Elevated leaching is simulated in coastal regions of East Asia, the eastern Atlantic Ocean and the northern Indian Ocean. However, the contribution of plastics to seawater concentrations remains relatively minor compared with direct riverine inputs and atmospheric deposition[53,54]. For example, observed PAE concentrations are 562–1,460 ng l^{-1} in the Pearl River Delta and 12–61 ng l^{-1} in the South China Sea[35,55], while the plastic leaching concentration is 0.1–0.5 ng l^{-1} (Supplementary Fig. 10a), accounting for just 0.03–0.8%. In the open ocean, PAEs from plastics contribute ~0.01 ng l^{-1} (Fig. 5a). Existing observational data on BPA primarily focus on nearshore areas, with concentrations ranging from 1.32 to 20.8 ng l^{-1} in the East China Sea and from 4.8 to 40 ng l^{-1} in the North Sea[56,57]. Our calculation suggests that the contribution of the additive leaching source may be around 1.3%–38% in these regions (Supplementary Fig. 10b, c). The modelled excess concentration of BPA from plastics ranges from 0.1 to 1 ng l^{-1} in the open ocean (Fig. 5b). Observed BPA concentrations are typically below detection limits in offshore waters (for example, the North Sea), possibly due to river dilution or the short half-life of BPA. Plastic release may emerge as a more important source for BPA in the remote open ocean, thereby highlighting the conveyance effect of plastics for these additives. We evaluate exposure risks of additives for organisms, with spatial patterns varying by organism size and additive distribution.

https://doi.org/10.1038/s41893-025-01620-x

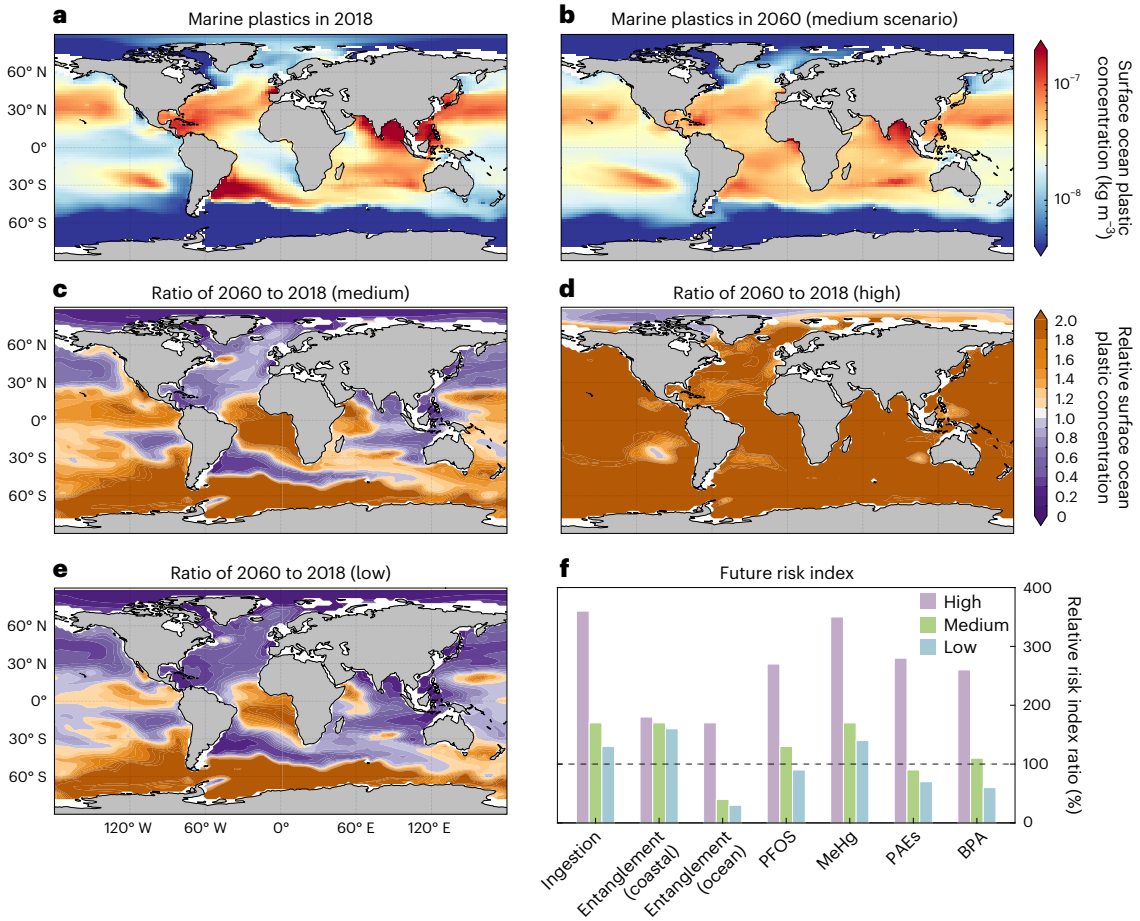

Fig. 6 | Marine plastic concentration and risk index ratios across various pathways between 2060 and 2018. a, Plastic concentration in 2018. **b**, Plastic concentration in 2060 under medium scenario. **c**, Ratio of plastic concentration in 2060 to that in 2018 under the medium scenario. **d**, Ratio of plastic concentration in 2060 to that in 2018 under the high scenario. **e**, Ratio of plastic concentration in 2060 to that in 2018 under the low scenario. **f**, Relative risk index ratios for ingestion risk, entanglement risk in coastal areas, entanglement risk in the open ocean, exposure risk for adsorbed PFOS, exposure risk for adsorbed MeHg, exposure risk for leached PAEs and exposure risk for leached BPA between 2060 and 2018 under the three scenarios. The risk for 2018 serves as the 100% baseline, with future scenario risks expressed as percentages relative to the 2018 risk index. Basemaps in **a**–**e** from Natural Earth (https://www.naturalearthdata.com).

Hotspots are in the mid-latitude Atlantic, North Pacific, northern Indian Ocean and coastal East Asia. The BPA leaching concentration is much lower than the estimated acute hazardous concentration for estuarine and marine species (HC_5 = 1.18 mg l^{-1}), as well as the 72-h median lethal concentration (LC_{50} = 20.9 mg l^{-1}) and median effect concentration (EC_{50} = 9.7 mg l^{-1}) for zebrafish larvae[58,59].

Future projections

We consider three emission scenarios with high, medium and low levels of global plastic discharges to project future changes in marine plastic concentrations and their associated risks (Fig. 6). The high scenario assumes no improvement in global waste management. The medium scenario reflects enhanced management efforts, while the low scenario further incorporates reductions in plastic use[60]. Plastic discharges from fisheries and shipping follow the same trend as riverine inputs and account for 25% of total terrestrial emissions in all scenarios (Methods and Supplementary Section 2).

Under the medium-emission scenario, plastic concentrations are projected to decline by 23% in the North Atlantic, 33% in the North Pacific and 24% in the Indian Ocean. In contrast, concentrations increase by 78% in the southeastern Atlantic and 41% in the South Pacific due to rising emissions from Africa and South America. Globally, plastic concentrations under the high-emission scenario are 2.8 times higher than in 2018, whereas the low-emission scenario results in concentrations that are, on average, 24% lower than those under the medium scenario (Fig. 6a–e and Supplementary Section 3).

Changes in plastic risks generally follow emission trends, but they are also influenced by biomass distribution, leading to pronounced regional variability. Without mitigation, ingestion risk is projected to increase by 360% relative to 2018. This increase can be limited to 170% or 130% with control measures (Fig. 6f). In the low-emission scenario, ingestion risk declines in the North Atlantic and North Pacific but increases in the Southern Hemisphere (Supplementary Fig. 15 and Supplementary Section 4). Entanglement risk in the open ocean is highly sensitive to ocean-sourced macroplastic levels, decreasing to 40% and 30% of 2018 values under the medium- and low-emission scenarios, respectively. However, entanglement risk in coastal regions continues to rise due to the long-term accumulation of plastic on beaches (Supplementary Figs. 16 and 17). Exposure risks from hazardous substances leached from or adsorbed onto plastics vary across regions and scenarios. The exposure risk index for adsorbed PFOS reaches 270%, 130% and 90% of 2018 levels under the three scenarios, while that for MeHg reaches 350%, 170% and 140%. Risks increase substantially in the South Pacific, South Atlantic and western Indian Ocean (Supplementary Figs. 18 and 19). MeHg exposure remains elevated across all scenarios due to high biological sensitivity in equatorial and southern oceans.

Exposure risk indices for the plastic additives BPA and PAEs fall below 2018 levels under the low-emission scenario.

Implications of sustainability

We employ a semiquantitative method to assess ecological risks of marine plastic pollution and map their spatial distribution across the global ocean. Our results can provide guidance for alleviating the ecological risk caused by marine plastics. The cleanup of plastic debris from oceans and waterways has been recognized as an efficient mitigation measure against plastic threats[61]. For instance, The Ocean Cleanup employs a cleanup system to capture plastic debris in the Great Pacific Garbage Patch and deploys interceptors to capture river-borne plastics[62]. However, plastic remediation technologies may result in potential bycatch, increased costs and ecological impacts[61,63]. Therefore, we suggest that in the cleanup efforts, in addition to the garbage patch, oceanic areas with higher risk probabilities, such as the mid-latitude Atlantic Ocean, mid-latitude North Pacific, northern Indian Ocean and coastal regions could be taken into account. Moreover, beaches represent key overlap zones characterized by dense plastic waste accumulation and frequent human activities[64]. Engaging the public in beach cleanup initiatives through community-led efforts offers a feasible approach[65]. Meanwhile, plastic has permeated the Arctic Ocean and food web therein, posing potential ecological risks that necessitate further research and attention[66].

Our study underscores the fact that limiting the release of large plastic debris, particularly ghost fishing gear in the coastal and nearshore areas, is an urgent mitigation measure to reduce entanglement risk for marine organisms. Rescue efforts in these regions are also critical, as they are recognized hotspots of entanglement risk. While biodegradable gear has the potential to reduce entanglement incidents due to lower environmental persistence, its degradation may increase ingestion risks and promote the adsorption of contaminants owing to a high affinity for organic pollutants[67].

Our simulations of future scenarios indicate that reducing mismanaged plastic waste (MPW) on land has a substantial impact on future oceanic plastic concentrations and their associated ecological risks. In the emission reduction scenario, risks associated with entanglement in the open ocean, biological exposure to contaminations adsorbed onto plastics and exposure to plastic additives are all decreased. However, rising emissions from Africa and other regions offset these improvements, resulting in elevated risks in the Southern Hemisphere. This underscores the need for a coordinated global response, with all continents implementing more aggressive and sustained emission reduction measures. The ongoing negotiations for a global plastic pollution treaty are therefore pivotal, and our research provides a comprehensive framework for assessing plastic risk, offering insights for designing more cost-effective risk mitigation policies and actions.

We have assessed the relative risks posed by marine plastics through four pathways and projected their potential changes under future emission scenarios. This approach lays the foundation for informed management and policy development aimed at mitigating the escalating threat of plastic pollution. Our results reveal distinct spatial risk patterns, with hotspots in regions such as the North Pacific and North Atlantic oceans, and demonstrate that plastics can serve as conveyors of chemical contaminants through adsorption, leaching and transformation processes. Additionally, we analyse uncertainties in our risk evaluation across multiple dimensions, including model parameters, assessment methods and observational data (Supplementary Section 5). However, our utilization of the risk index suggests that the relative probability of risk occurrence in space lacks the ability to represent realistic endpoints such as death or illness, and the variation in assessment methods across different risk pathways poses challenges to direct comparisons between risks. Thus, we advocate that the evaluation model should be refined by integrating additional factors, including pollutant adsorption capacity, additive leaching and the physiological impacts of plastic–pollutant complexes. Moreover, a unified risk framework is needed to quantitatively compare across risk pathways and incorporate data on mortality and morbidity from marine populations[68,69]. Future research should also prioritize establishing dose–effect relationships specific to marine plastics, expanding observational efforts in high-risk regions to validate model outputs and incorporating laboratory-derived kinetic parameters to reduce uncertainties. These improvements will considerably enhance the accuracy and robustness of global plastic pollution risk assessments.

Methods

Ocean plastic model

We utilize the NJU-MP model, a simulation framework developed by Zhang et al.[32], based on the MITgcm. The model encompasses 22 vertical levels and operates at a horizontal resolution of 2° latitude × 2.5° longitude. It incorporates five distinct chemical compositions: PE (950 kg m^{-3}), PP (900 kg m^{-3}), PVC (1,410 kg m^{-3}), PS (1,050 kg m^{-3}) and ABS (1,050 kg m^{-3}). Microplastics are categorized into four size bins (<0.078 mm, 0.0781–0.3125 mm, 0.3125–1.25 mm and 1.25–5 mm) and macroplastics into two size bins (5–50 mm and >50 mm). Plastic sources include riverine emission inventory data from Mai et al.[70]. Additionally, the model considers direct ocean emissions resulting from marine activities such as shipping and fishing, accounting for 25% of terrestrial discharge[43,71]. The NJU-MP model simulates the dynamic process of plastic in the ocean, including drifting, sinking, beaching and biofouling. Light particles, such as PP and PE, exhibit quasi-two-dimensional drifting behaviour near the ocean surface. In contrast, higher-density particles (PVC, PS, ABS), tend to sink after being dumped. The sinking or rising of particles is approximated as one-dimensional motion relative to the water column. The model also uses fragmentation rate and beach datasets to simulate the degradation process and the probability of plastics being beached on sandy shores[72,73]. To improve model accuracy, data assimilation is applied using a three-dimensional variational method to optimize global plastic emissions to oceans, on the basis of previous emission estimates and seawater plastic observations. The optimization is performed on model instances that form a super-ensemble. This ensemble includes 50 models generated via a Monte Carlo approach, with two additional models representing the extreme values of the parameters. Each model is run with three different emission inventories from Lebreton et al.[2], Mai et al.[70] and Weiss et al.[74], resulting in a total of 156 model members. The optimization process is repeated for all 156 members, yielding an ensemble of best-estimate emissions. Additionally, observed data are used to refine modelled surface plastic concentrations[32].

We use the future plastic emission inventory and the NJU-MP model to project future marine plastic distributions. Three emission scenarios (high, medium and low) are established according to Lebreton and Andrady[60], in which the proportion of MPW is negatively related to the per capita gross domestic product, reflecting the fact that the management level of plastic waste has improved with economic growth. The high scenario assumes that current waste management practices will continue in various countries, resulting in an increase in the total amount of MPW. The medium scenario incorporates enhanced waste management efforts as per capita gross domestic product increases and a projected shift in global MPW from Asia to Africa. Under this scenario, total MPW generation would peak before 2020 and then decrease. The low scenario builds on the medium scenario, envisioning further reductions in household plastic use to 10% of municipal solid waste by 2020 and 5% by 2040[60]. We sum the MPW quantities for major countries across the six continents under three scenarios for the years 2020, 2040 and 2060. Emission trends and rates of increase or decrease are then fitted to scale our own future plastic emission inventory (Supplementary Fig. 14). The model operates from 1950 to 2060. In addition to riverine emissions, adjustments for direct ocean-source emissions follow the same trend as for riverine inputs, accounting for 25% of terrestrial discharge across all

three scenarios[32]. The simulation of plastic dynamics remains consistent with previous studies. Drifting velocities of light particles in the surface ocean and solar radiation data, which are related to the fragmentation rates of surface plastics, are used from 2009 to 2018 and cycled every ten years to project future conditions[75].

Ocean ecosystem model

We employ ocean biomass data from the NEMO-PISCES-APECOSM model, which couples ocean dynamics with ecosystem processes[76,77]. Within this framework, NEMO-PISCES simulates biogeochemical cycles, including phytoplankton, zooplankton and particulate organic matter, providing foundational input to APECOSM. APECOSM builds upon this by resolving three-dimensional, size-structured ecosystem dynamics, guided by the dynamic energy budget theory[78], which is rooted in ecological and physiological principles and emphasizes the conservation of mass and energy. The model incorporates various ecological processes, including size-based opportunistic trophic interactions, predator competition for food, energy allocation for growth and reproduction, somatic maintenance and maturation, predation, starvation and other natural mortality factors[33,79].

The model simulates a dynamic size structure of the marine ecosystem by representing the distribution of energy content across organism weight classes, particularly at the highest trophic level, where energy is assumed to be proportional to biomass[33]. The upper trophic levels in APECOSM are categorized into three distinct open ocean pelagic communities. Specifically, the open ocean epipelagic community spans the sea surface to 200 m, and the mesopelagic community occupies the middle ocean (200–1,000 m). The migratory open ocean pelagic community performs diel vertical migrations, feeding in the surface ocean at night and retreating to the mesopelagic layer during the day. Each community is further divided into 20 size classes ranging from 1 mm to almost 2 m (1 mm, 2 mm, 3 mm, 4 mm, 6 mm, 9 mm, 13 mm, 18 mm, 27 mm, 39 mm, 58 mm, 84 mm, 123 mm, 180 mm, 263 mm, 385 mm, 562 mm, 823 mm, 1,203 mm, 1,759 mm), encompassing mesozooplankton to large fish. To estimate biomass, we multiply the original energy values by the weights of the 20 size classes and then divide by the specific free energy of biomass, defined as 474.6 kJ mol C^{-1}, where mol C refers to moles of carbon[33,78,80].

PFOS and MeHg data

We utilize the PFOS concentration data in the global ocean as modelled by Zhang et al.[48]. This model incorporates tracers for both dissolved and particle-bound forms of PFOS, boasting a spatial resolution of 1° × 1° and 23 vertical levels. It accounts for the lateral and vertical transport of PFOS through oceanic circulation, mixing and particle settling. The temporal dynamics of PFOS inventory span from 1958 to 2010, originating from wastewater treatment plants and rivers in the North America and Europe. Before 1958, PFOS concentrations are designated as zero. Between 1958 and 2010, historical inventories are employed to supply grid inputs for the North Atlantic region, within the latitude range of 20–60° N. The simulation encompasses the phase-out of PFOS production, featuring zero inputs from 2010 to 2038.

The MeHg data employed in our study are sourced from the model developed by Zhang et al.[49], which comprehensively simulates its biogeochemical cycling, including chemical transformation, transport and trophic transfer within the MITgcm framework. In this advanced model, CH_3Hg and $(CH_3)_2Hg$ are introduced as tracers. The formation of MeHg predominantly depends on the simulated behaviour of inorganic mercury, with the methylation rate dynamically adjusted on the basis of environmental parameters, ultimately yielding its concentration in seawater. The model considers two primary degradation mechanisms. The first is photochemical demethylation driven by shortwave radiation, and the second is dark demethylation mediated by biological activity and other abiotic processes. Moreover, both the PFOS and MeHg models are constrained by observational datasets, ensuring their reliability and accuracy in capturing real-environmental dynamics.

Ingestion risk

The risk of plastic ingestion is influenced by various factors, including plastic exposure, habitat and the body size of organisms[9,10]. Among these factors, the ratio between the body length of the organism and the diameter of the plastic is easily accessible information. An approximate 20:1 ratio exists between the body length of an organism and the maximum ingestible plastic diameter[11]. Obtaining information regarding the habitat range of organisms poses a challenge, given that each category in the ecosystem model encompasses multiple species. To address this limitation, the ingestion probability is estimated by defining it as the product of the body size of the organism and the concentration of plastics within the ingestible size range. Organisms with body size exceeding 1,203 mm are considered capable of ingesting plastics across all particle size categories defined in the model (Supplementary Table 1). The probability of plastic ingestion is calculated as follows:

$$\text{Ingestion risk} = \text{MP}_{\text{max}} \times \text{Biomass} \quad (1)$$

where MP_{max} denotes the sum of the concentrations of all plastics within the maximum ingestible diameter. We use the vertical mean concentration of plastics within the top 200 m of the ocean to calculate the ingestion risk for epipelagic organisms. For mesopelagic organisms the depth range is 200–800 m, and for migratory organisms 0–800 m. 'biomass' indicates the biomass of marine organisms in 20 sizes.

The correlation between the body size of an organism and its maximum diameter of ingestible plastic is established through a survey of 2,000 wild animals and statistical methods[11]. This correlation can be expressed by the following equation:

$$\text{Plastic size} = 10^{0.934 \log_{10}(\text{Body size}) - 1.1200}. \quad (2)$$

Entanglement risk

Given the absence of standardized methodologies and the limited availability of data on entanglement rates and body sizes for marine organisms, we adopt the analytical framework proposed by Wilcox et al., originally developed to assess sea turtle entanglement caused by ghost nets in northern Australia[81]. In this framework, entanglement risk is influenced by the frequency of encounters between organisms and debris, and the relative encounter rates of debris across species play an important role in the assessment. We estimate entanglement risk by multiplying macroplastic concentrations (>5 cm) from fishing and shipping sources, particularly ALDFG, by the biomass of organisms vulnerable to entanglement. Observational evidence demonstrates a strong correlation between ALDFG and instances of plastic entanglement[16,46]. Simulated concentrations are specifically incorporated for PP, PE and PVC, given their prevalent use in the production of fishing nets, lines and traps[16,82]. Our analysis focuses on marine organisms with body sizes exceeding 180 mm (such as large fish) to assess the entanglement risk. Organisms with a size smaller than 180 mm are excluded due to limited entanglement records and their low susceptibility to entanglement[19,46]. The entanglement risk is calculated as follows:

$$\text{Entanglement risk} = \text{MP}_{>5.0\,\text{cm}} \times \text{Biomass}_{180.0\,\text{mm}-1{,}759.0\,\text{mm}} \quad (3)$$

where $\text{Biomass}_{180.0\,\text{mm}-1{,}759.0\,\text{mm}}$ represents the biomass of the organisms with body lengths from 180 mm to 1,759 mm and $\text{MP}_{>5.0\,\text{cm}}$ is the concentration of PE, PP and PVC plastics with a diameter larger than 5 cm.

Pollution conveyor risk

We use the equilibrium partition coefficients of PFOS between seawater and plastics to calculate the concentration of PFOS absorbed by plastics:

$$C_{\text{PFOS}}^{\text{Plastic}} = C_{\text{PFOS}}^{\text{Seawater}} K_{\text{d}} C_{\text{Plastic}}^{\text{Seawater}} \quad (4)$$

where $C_{PFOS}^{Plastic}$ represents the concentration of PFOS adsorbed by the plastic and $C_{PFOS}^{Seawater}$ and $C_{Plastic}^{Seawater}$ denote the concentrations of PFOS and plastics in the ocean. The value of K_d varies with the diameter of the plastic. To ascertain K_d values, we utilize MATLAB to fit the experimentally derived K_d values for PP and assume that the K_d for PE is identical to that of PP[26,27]. K_d is 100.5 l kg^{-1} for PVC[27]. However, the K_d values for PS and ABS remain ambiguous. We multiply the organic carbon-normalized partition coefficient (log K_{oc} = 2.6) by the organic carbon fraction (f_{oc}) of PS (0.923) and ABS (0.853) to estimate these values[83].

Due to the lack of experimental data, the K_d of MeHg between seawater and plastic is still uncertain. We regard plastic as organic matter, and the calculation of the concentration of MeHg absorbed by plastics can be performed as follows:

$$C_{CH_3Hg}^{Plastic} = C_{CH_3Hg}^{Seawater} K_{oc} f_{oc} C_{Plastic}^{Seawater} \quad (5)$$

where $C_{CH_3Hg}^{Plastic}$ is the concentration of MeHg absorbed by plastics in the ocean, K_{oc} is the partition coefficient of CH_3Hg ($K_d = 6.3 \times 10^3$ l kg^{-1})[49] and f_{oc} is the organic content of plastics (PE, 0.857; PP, 0.857; PVC, 0.384; PS, 0.923; ABS, 0.853).

Additive leaching risk

We quantify the concentrations of two ubiquitous plastic additives, BPA and PAEs, commonly detected in marine plastics and subsequently leached into seawater. The mass fraction of BPA in PP and PE ranges from 0.3% to 3% (ref. 84), with the median fraction of 1.58% selected to calculate the mass content. We assume a consistent content ratio in PS and ABS. For PVC, the BPA content varies from 0.5% to 3%, thus we opt for 1.75% as a representative value. Concerning PAEs, the content ratio within PVC ranges from 30% to 70% (ref. 84), and we utilize the mean fraction of 35% in our estimation[85]. Given that PAEs are added in lesser quantities to other plastics, the fractions in PE, PP, PS and ABS are determined by dividing the global production of PAEs (5.8 million tons) in 2021 by the worldwide production of plastics (335 million tons)[86], resulting in a proportion of 0.15%. The overall additive content is calculated as follows:

$$M_{additive} = \sum_i \omega_i M_i \ (i: \text{PP, PE, PVC, PS, ABS}) \quad (6)$$

where $M_{additive}$ represents the total mass of PAEs and BPA contained in the plastic, ω_i represents the mass fraction of additives in various types of plastic and M_i denotes the mass of the plastic.

The total additive leaching mass is calculated by multiply the leaching rate by the plastic mass. The additive leaching concentration is calculated by multiplying the leaching ratio of plastic additives by mass and the plastic concentration in the ocean:

$$Q_{additive} = k_{additive} M_{plastic} \quad (7)$$

$$C_{additive} = r_{additive} \omega C_{plastic} \quad (8)$$

where k is the leaching rate. For PAEs, the leaching rate is set as 58.4 μg kg^{-1} d^{-1} for PE, 9.05 μg kg^{-1} d^{-1} for PP and 253 μg kg^{-1} d^{-1} for PVC[86,87]. For BPA from PVC and PS, average leaching rates are approximately 11.7 mg kg^{-1} d^{-1} and 231 mg kg^{-1} d^{-1}, respectively[51,52]. The leaching ratios of PAEs for PE, PP and PVC are 1.44%, 0.216% and 0.0256%, respectively. For PVC and PS, the leaching ratios of BPA are 3.8% and 38%, respectively.

Reporting summary

Further information on research design is available in the Nature Portfolio Reporting Summary linked to this article.

Data availability

Data are available in the text, in Supplementary Information or on the website. Plastic data are available at https://www.ebmg.online/plastics/plastic. The biomass datasets are available via Zenodo at https://zenodo.org/records/1460596 (ref. 77).
PFOS data are available at https://www.ebmg.online/plastics/PFOS.
MeHg data are available at https://www.ebmg.online/plastics/MeHg.

Code availability

All model code is available at the research group website: https://www.ebmg.online/plastics/MITgcm-code.

References

1. Haward, M. Plastic pollution of the world's seas and oceans as a contemporary challenge in ocean governance. *Nat. Commun.* **9**, 667 (2018).
2. Lebreton, L. C. M. et al. River plastic emissions to the world's oceans. *Nat. Commun.* **8**, 15611 (2017).
3. Bergmann, M., Sandhop, N., Schewe, I. & D'Hert, D. Observations of floating anthropogenic litter in the Barents Sea and Fram Strait, Arctic. *Polar Biol.* **39**, 553–560 (2016).
4. Gall, S. C. & Thompson, R. C. The impact of debris on marine life. *Mar. Pollut. Bull.* **92**, 170–179 (2015).
5. Savoca, M. S., McInturf, A. G. & Hazen, E. L. Plastic ingestion by marine fish is widespread and increasing. *Glob. Change Biol.* **27**, 2188–2199 (2021).
6. Gilbert, J. M., Reichelt-Brushett, A. J., Bowling, A. C. & Christidis, L. Plastic ingestion in marine and coastal bird species of southeastern Australia. *Mar. Ornithol.* **44**, 21–26 (2016).
7. Ryan, P. G. Intraspecific variation in plastic ingestion by seabirds and the flux of plastic through seabird populations. *Condor* **90**, 446–452 (1988).
8. Puskic, P. S., Lavers, J. L. & Bond, A. L. A critical review of harm associated with plastic ingestion on vertebrates. *Sci. Total Environ.* **743**, 140666 (2020).
9. Wilcox, C., Van Sebille, E. & Hardesty, B. D. Threat of plastic pollution to seabirds is global, pervasive, and increasing. *Proc. Natl Acad. Sci. USA* **112**, 11899–11904 (2015).
10. Compa, M. et al. Risk assessment of plastic pollution on marine diversity in the Mediterranean Sea. *Sci. Total Environ.* **678**, 188–196 (2019).
11. Jâms, I. B., Windsor, F. M., Poudevigne-Durance, T., Ormerod, S. J., & Durance, I. Estimating the size distribution of plastics ingested by animals. *Nat. Commun.* **11**, 1594 (2020).
12. Pegado, T. D. E. S. et al. First evidence of microplastic ingestion by fishes from the Amazon River estuary. *Mar. Pollut. Bull.* **133**, 814–821 (2018).
13. Senko, J. F. et al. Understanding individual and population-level effects of plastic pollution on marine megafauna. *Endanger. Species Res.* **43**, 234–252 (2020).
14. Stelfox, M., Hudgins, J. & Sweet, M. A review of ghost gear entanglement amongst marine mammals, reptiles and elasmobranchs. *Mar. Pollut. Bull.* **111**, 6–17 (2016).
15. Gilman, E., Chopin, F., Suuronen, P. & Kuemlangan, B. *Abandoned, Lost and Discarded Gillnets and Trammel Nets: Methods to Estimate Ghost Fishing Mortality, and the Status of Regional Monitoring and Management* Fisheries and Aquaculture Technical Paper 600, 1–59, 61–79, IV (FAO, 2016).
16. Wilcox, C., Mallos, N. J., Leonard, G. H., Rodriguez, A. & Hardesty, B. D. Using expert elicitation to estimate the impacts of plastic pollution on marine wildlife. *Mar. Policy* **65**, 107–114 (2016).
17. McIntosh, R. R., Kirkwood, R., Sutherland, D. R. & Dann, P. Drivers and annual estimates of marine wildlife entanglement rates: a long-term case study with Australian fur seals. *Mar. Pollut. Bull.* **101**, 716–725 (2015).

18. Afonso, A. S. & Fidelis, L. The fate of plastic-wearing sharks: entanglement of an iconic top predator in marine debris. *Mar. Pollut. Bull.* **194**, 115326 (2023).
19. Duncan, E. M. et al. A global review of marine turtle entanglement in anthropogenic debris: a baseline for further action. *Endanger. Species Res.* **34**, 431–448 (2017).
20. Rodríguez, Y. et al. Litter ingestion and entanglement in green turtles: an analysis of two decades of stranding events in the NE Atlantic. *Environ. Pollut.* **298**, 118796 (2022).
21. Prunier, J. et al. Trace metals in polyethylene debris from the North Atlantic subtropical gyre. *Environ. Pollut.* **245**, 371–379 (2019).
22. Zhan, Z. W. et al. Sorption of 3,3′,4,4′-tetrachlorobiphenyl by microplastics: a case study of polypropylene. *Mar. Pollut. Bull.* **110**, 559–563 (2016).
23. Islam, N. et al. Perfluorooctane sulfonic acid (PFOS) adsorbed to polyethylene microplastics: accumulation and ecotoxicological effects in the clam. *Mar. Environ. Res.* **164**, 105249 (2021).
24. Zhu, J. et al. Effects of microplastics on the accumulation and neurotoxicity of methylmercury in zebrafish larvae. *Mar. Environ. Res.* **176**, 105615 (2022).
25. Teuten, E. L. et al. Transport and release of chemicals from plastics to the environment and to wildlife. *Philos. Trans. R. Soc. B* **364**, 2027–2045 (2009).
26. Cormier, B. et al. Sorption and desorption kinetics of PFOS to pristine microplastic. *Environ. Sci. Pollut. Res.* **29**, 4497–4507 (2022).
27. Wang, F., Shih, K. M. & Li, X. Y. The partition behavior of perfluorooctanesulfonate (PFOS) and perfluorooctanesulfonamide (FOSA) on microplastics. *Chemosphere* **119**, 841–847 (2015).
28. Guerrini, F., Mari, L. & Casagrandi, R. A coupled Lagrangian–Eulerian model for microplastics as vectors of contaminants applied to the Mediterranean Sea. *Environ. Res. Lett.* **17**, 024038 (2022).
29. Fauser, P., Vorkamp, K. & Strand, J. Residual additives in marine microplastics and their risk assessment—a critical review. *Mar. Pollut. Bull.* **177**, 113467 (2022).
30. Oehlmann, J. et al. A critical analysis of the biological impacts of plasticizers on wildlife. *Philos. Trans. R. Soc. B* **364**, 2047–2062 (2009).
31. Hoiberg, M. A., Woods, J. S. & Verones, F. Global distribution of potential impact hotspots for marine plastic debris entanglement. *Ecol. Indic.* **135**, 108509 (2022).
32. Zhang, Y. X. et al. Plastic waste discharge to the global ocean constrained by seawater observations. *Nat. Commun.* **14**, 1372 (2023).
33. Maury, O. et al. Modeling environmental effects on the size-structured energy flow through marine ecosystems. Part 1: The model. *Prog. Oceanogr.* **74**, 479–499 (2007).
34. Guo, R. X. et al. Bioaccumulation and elimination of bisphenol a (BPA) in the alga and the potential for trophic transfer to the rotifer. *Environ. Pollut.* **227**, 460–467 (2017).
35. Mi, L. J. et al. Air–sea exchange and atmospheric deposition of phthalate esters in the South China Sea. *Environ. Sci. Technol.* **57**, 11195–11205 (2023).
36. Onink, V., Wichmann, D., Delandmeter, P. & van Sebille, E. The role of Ekman currents, geostrophy, and Stokes drift in the accumulation of floating microplastic. *J. Geophys. Res. Oceans* **124**, 1474–1490 (2019).
37. Gregg, W. W. & Conkright, M. E. Decadal changes in global ocean chlorophyll. *Geophys. Res. Lett.* **29**, 20-1–20-4 (2002).
38. Liang, Z., Letscher, R. T. & Knapp, A. N. Dissolved organic phosphorus concentrations in the surface ocean controlled by both phosphate and iron stress. *Nat. Geosci.* **15**, 651–657 (2022).
39. Cózar, A. et al. The Arctic Ocean as a dead end for floating plastics in the North Atlantic branch of the thermohaline circulation. *Sci. Adv.* **3**, e1600582 (2017).
40. Collard, F. & Ask, A. Plastic ingestion by Arctic fauna: a review. *Sci. Total Environ.* **786**, 147462 (2021).
41. Clere, I. K. et al. Quantification and characterization of microplastics in commercial fish from southern New Zealand. *Mar. Pollut. Bull.* **184**, 114121 (2022).
42. Grosvik, B. E. et al. Assessment of marine litter in the Barents Sea, a part of the Joint Norwegian Russian Ecosystem Survey. *Front. Mar. Sci.* **5**, 72 (2018).
43. Kroodsma, D. A. et al. Tracking the global footprint of fisheries. *Science* **359**, 904–907 (2018).
44. Watson, R. A. & Tidd, A. Mapping nearly a century and a half of global marine fishing: 1869–2015. *Mar. Policy* **93**, 171–177 (2018).
45. Perez-Venegas, D. J. et al. Towards understanding the effects of oceanic plastic pollution on population growth for a South American fur seal (*Arctocephalus australis australis*) colony in Chile. *Environ. Pollut.* **279**, 116881 (2021).
46. Parton, K. J., Galloway, T. S. & Godley, B. J. Global review of shark and ray entanglement in anthropogenic marine debris. *Endanger. Species Res.* **39**, 173–190 (2019).
47. Perez-Venegas, D. J., Hardesty, B. D., Wilcox, C. & Galbán-Malagón, C. The hotspots of entanglement for pinnipeds of the world. *Mar. Pollut. Bull.* **195**, 115491 (2023).
48. Zhang, X. M., Zhang, Y. X., Dassuncao, C., Lohmann, R. & Sunderland, E. M. North Atlantic Deep Water formation inhibits high Arctic contamination by continental perfluorooctane sulfonate discharges. *Glob. Biogeochem. Cycles* **31**, 1332–1343 (2017).
49. Zhang, Y. X., Soerensen, A. L., Schartup, A. T. & Sunderland, E. M. A global model for methylmercury formation and uptake at the base of marine food webs. *Glob. Biogeochem. Cycles* **34**, e2019GB006348 (2020).
50. Chubarenko, I., Bagaev, A., Zobkov, M. & Esiukova, E. On some physical and dynamical properties of microplastic particles in marine environment. *Mar. Pollut. Bull.* **108**, 105–112 (2016).
51. Suhrhoff, T. J. & Scholz-Böttcher, B. M. Qualitative impact of salinity, UV radiation and turbulence on leaching of organic plastic additives from four common plastics—a lab experiment. *Mar. Pollut. Bull.* **102**, 84–94 (2016).
52. Gulizia, A. M. et al. Understanding plasticiser leaching from polystyrene microplastics. *Sci. Total Environ.* **857**, 159099 (2023).
53. Cao, Y. R. et al. Significant riverine inputs of typical plastic additives—phthalate esters from the Pearl River Delta to the northern South China Sea. *Sci. Total Environ.* **849**, 157744 (2022).
54. Net, S., Sempéré, R., Delmont, A., Paluselli, A. & Ouddane, B. Occurrence, fate, behavior and ecotoxicological state of phthalates in different environmental matrices. *Environ. Sci. Technol.* **49**, 4019–4035 (2015).
55. Paluselli, A. & Kim, S. K. Horizontal and vertical distribution of phthalates acid ester (PAEs) in seawater and sediment of East China Sea and Korean South Sea: traces of plastic debris? *Mar. Pollut. Bull.* **151**, 110831 (2020).
56. Heemken, O. P., Reincke, H., Stachel, B. & Theobald, N. The occurrence of xenoestrogens in the Elbe river and the North Sea. *Chemosphere* **45**, 245–259 (2001).
57. Shi, J. H., Liu, X. W., Chen, Q. C. & Zhang, H. Spatial and seasonal distributions of estrogens and bisphenol A in the Yangtze River Estuary and the adjacent East China Sea. *Chemosphere* **111**, 336–343 (2014).
58. Naveira, C., Rodrigues, N., Santos, F. S., Santos, L. N. & Neves, R. A. F. Acute toxicity of bisphenol A (BPA) to tropical marine and estuarine species from different trophic groups. *Environ. Pollut.* **268**, 115911 (2021).
59. Chen, X. N., Hang, X. M., Ke, W. B., Ma, Z. Y. & Sun, Y. Q. Acute and subacute toxicity of bisphenol A on zebrafish (*Danio rerio*). *Adv. Mater. Res.* **356–360**, 138–141 (2012).
60. Lebreton, L. & Andrady, A. Future scenarios of global plastic waste generation and disposal. *Palgrave Commun.* **5**, 6 (2019).

61. Falk-Andersson, J., Haarr, M. L. & Havas, V. Basic principles for development and implementation of plastic clean-up technologies: what can we learn from fisheries management? *Sci. Total Environ.* **745**, 141117 (2020).
62. 2024: A record-breaking year for The Ocean Cleanup. *The Ocean Cleanup* https://theoceancleanup.com/updates/2024-a-record-breaking-year-for-the-ocean-cleanup/ (2024).
63. Falk-Andersson, J. et al. Cleaning up without messing up: maximizing the benefits of plastic clean-up technologies through new regulatory approaches. *Environ. Sci. Technol.* **57**, 13304–13312 (2023).
64. Onink, V., Jongedijk, C. E., Hoffman, M. J., van Sebille, E. & Laufkötter, C. Global simulations of marine plastic transport show plastic trapping in coastal zones. *Environ. Res. Lett.* **16**, 064053 (2021).
65. Purba, N. P. et al. Coastal clean-up in Southeast Asia: lessons learned, challenges, and future strategies. *Front. Mar. Sci.* **10**, 1250736 (2023).
66. Bergmann, M. et al. Plastic pollution in the Arctic. *Nat. Rev. Earth Environ.* **3**, 323–337 (2022).
67. Wilcox, C. & Hardesty, B. D. Biodegradable nets are not a panacea, but can contribute to addressing the ghost fishing problem. *Anim. Conserv.* **19**, 322–323 (2016).
68. Hardesty, B. D. & Wilcox, C. A risk framework for tackling marine debris. *Anal. Methods* **9**, 1429–1436 (2017).
69. Roman, L., Hardesty, B. D. & Schuyler, Q. A systematic review and risk matrix of plastic litter impacts on aquatic wildlife: a case study of the Mekong and Ganges river basins. *Sci. Total Environ.* **843**, 156858 (2022).
70. Mai, L. et al. Global riverine plastic outflows. *Environ. Sci. Technol.* **54**, 10049–10056 (2020).
71. Lebreton, L. C. M., Greer, S. D. & Borrero, J. C. Numerical modelling of floating debris in the world's oceans. *Mar. Pollut. Bull.* **64**, 653–661 (2012).
72. Welden, N. A. & Cowie, P. R. Degradation of common polymer ropes in a sublittoral marine environment. *Mar. Pollut. Bull.* **118**, 248–253 (2017).
73. Luijendijk, A. et al. The state of the world's beaches. *Sci. Rep.* **8**, 6641 (2018).
74. Weiss, L. et al. The missing ocean plastic sink: gone with the rivers. *Science* **373**, 107–111 (2021).
75. Biber, N. F. A., Foggo, A. & Thompson, R. C. Characterising the deterioration of different plastics in air and seawater. *Mar. Pollut. Bull.* **141**, 595–602 (2019).
76. Aumont, O., Maury, O., Lefort, S. & Bopp, L. Evaluating the potential impacts of the diurnal vertical migration by marine organisms on marine biogeochemistry. *Glob. Biogeochem. Cycles* **32**, 1622–1643 (2018).
77. Aumont, O., Maury, O., Bopp, L. & Lefort, S. Dataset and code of NEMO-PISCES-APECOSM. *Zenodo* https://doi.org/10.5281/zenodo.1460596 (2018).
78. Koojiman, S. A. L. M. *Dynamic Energy and Mass Budgets in Biological Systems* (Cambridge Univ. Press, 2000).
79. Maury, O., Shin, Y. J., Faugeras, B., Ben Ari, T. & Marsac, F. Modeling environmental effects on the size-structured energy flow through marine ecosystems. Part 2: Simulations. *Prog. Oceanogr.* **74**, 500–514 (2007).
80. Lefort, S. et al. Spatial and body-size dependent response of marine pelagic communities to projected global climate change. *Glob. Change Biol.* **21**, 154–164 (2015).
81. Wilcox, C. et al. Ghostnet impacts on globally threatened turtles, a spatial risk analysis for northern Australia. *Conserv. Lett.* **6**, 247–254 (2013).
82. Keskin, I. & Ekici, A. Effects of environmental factors and food availability in Northern Aegean sea on the cultivation of Mediterranean mussels (*Mytilus galloprovincialis*). *Aquac. Res.* **52**, 65–76 (2021).
83. Higgins, C. P. & Luthy, R. G. Sorption of perfluorinated surfactants on sediments. *Environ. Sci. Technol.* **40**, 7251–7256 (2006).
84. Hermabessiere, L. et al. Occurrence and effects of plastic additives on marine environments and organisms: a review. *Chemosphere* **182**, 781–793 (2017).
85. da Costa, J. P., Avellan, A., Mouneyrac, C., Duarte, A. & Rocha-Santos, T. Plastic additives and microplastics as emerging contaminants: mechanisms and analytical assessment. *Trends Anal. Chem.* **158**, 116898 (2023).
86. Cao, Y. R. et al. Microplastics: a major source of phthalate esters in aquatic environments. *J. Hazard. Mater.* **432**, 128731 (2022).
87. *Plastics—The Facts 2017: An Analysis of European Plastics Production, Demand and Waste Data* (Plastics Europe, 2016).

Acknowledgements

We acknowledge O. Aumont et al. for providing their data and insights, which substantially contributed to this research. The data utilized in this study were sourced from their article 'Evaluating the potential impacts of the diurnal vertical migration by marine organisms on marine biogeochemistry', published in *Global Biogeochemical Cycles*[76]. Additionally, we appreciate the support and contributions of M. Egger for his review and suggestions on our paper.

Author contributions

Y.Z. and Z.Z. conceived the study. Z.Z., P.W., X.W., Q.P. and X.Z. developed the methodology. Z.Z., P.W. and Y.W. performed the visualization. Y.Z. administered the project and provided overall supervision. Z.Z. and Y.Z. prepared the original draft of the manuscript. Y.Z., Z.Z., X.Z., E.Y.Z., K.K. and L.L. contributed to the review and editing of the manuscript.

Competing interests

The authors declare no competing interests.

Additional information

Extended data is available for this paper at https://doi.org/10.1038/s41893-025-01620-x.

Supplementary information The online version contains supplementary material available at https://doi.org/10.1038/s41893-025-01620-x.

Correspondence and requests for materials should be addressed to Yanxu Zhang.

Peer review information *Nature Sustainability* thanks Gabriel De la Torre, Valentina H. Pauna and the other, anonymous, reviewer(s) for their contribution to the peer review of this work.

https://doi.org/10.1038/s41893-025-01620-x

Extended Data Table 1 | Additive mass and leaching rates from ocean plastics in 2018

	Plastic mass ($\times 10^8$ kg)	BPA mass ($\times 10^6$ kg)	PAEs mass ($\times 10^5$ kg)	Leach rate of PAEs ($\times 10^3$ kgyear^{-1})	Leach rate of BPA ($\times 10^5$ kgyear^{-1})
PE	2.3	4.0	3.4	4.9	
PP	1.7	3.0	2.6	0.561	
PVC	1.5	2.7	539	13.8	1.0
PS	1.1	1.8	1.6		5.1
ABS	0.4	0.7	0.6		

Mass of plastic additives (PAEs and BPA) contained in different plastic types and their corresponding leaching rates into the ocean in 2018. Leaching rates are listed for PAEs in PP, PE, and PVC, and for BPA in PVC and PS.